eprints@whiterose.ac.uk
https://eprints.whiterose.ac.uk/

Vibration Control of Bridges Under Simultaneous Effects of Earthquake and Moving Loads Using Steel Pipe Dampers

Ali Nikkhoo [a], Ardalan Bahrami Eskandari [a], Ali Farazandeh [a], Iman Hajirasouliha [b]*

[a] Department of Civil Engineering, The University of Science and Culture, Tehran, Iran

[b] Department of Civil and Structural Engineering, The University of Sheffield, Sheffield, UK

* Corresponding author; Email: i.hajirasouliha@sheffield.ac.uk

Abstract

This study aims to develop a practical methodology based on Eigenfunction Expansion Method (EEM) to assess the effects of simultaneous action of vertical earthquake excitation and moving vehicle loads in single-span and multi-span simply supported bridges. While the effects of vertical earthquake ground motions are generally ignored in common design practice, it is shown that the influence of simultaneous vertical earthquake excitation and vehicle loads can considerably affect the structural response of the bridge, especially in near field earthquakes with high amplitude vertical components. To address this issue, a novel vibration suppression system is proposed using steel pipe dampers and the reliability of the system is investigated for a wide range of bridge flexural rigidity under seven different earthquake records. The results indicate that the proposed system can significantly (up to 75%) supress the vertical vibrations generated in the bridge, especially for the systems with lower flexural rigidity. It is also shown that, in general, the efficiency of the pipe dampers is improved by increasing the M_n and $V_s 30(m/s)$ of the input earthquake. For the same maximum deflection limits, application of pipe dampers could reduce (up to 50%) the required flexural rigidity of the bridge, and therefore, lead to a more economic design solution with lower structural weight.

Keywords: Bridge Vibration, Vibration Suppression, Vertical Earthquake Excitation, Moving Inertial Loads, Steel Pipe Damper

1. Introduction

Currently, most bridge design guidelines (e.g. The European Standard EN1991-2 1991; American Railway Engineering and Maintenance-of-Way Association (AREMA) 1997; Union Internationale des Chemins de Fer 2002) rely heavily on static analysis methods to account for the impact of vehicle and train loads. While such simplified approaches can be acceptable for conventional train systems, previous studies have demonstrated that more sophisticated methods may be required to obtain accurate results, especially in case

of long-span bridges traversed by high-speed loads (Nikkhoo et al. 2007; Kiani and Nikkhoo 2012; Maximov 2014; Karimi and Ziaei-Rad 2015; Salcher and Adam 2015; Yang et al. 2017; He 2018).

The structural response of linear continuous beams (representing conventional bridge systems) under dynamic loads has been a topic of many investigations (Ahmadi 1978; Su and Ahmadi 1988; Frýba 1999; Leissa and Qatu 2011; Ouyang 2011; Beskou and Theodorakopoulos 2011; Pi and Ouyang 2015; Zhu et al. 2015). However, most of these studies were limited to the beam vibrations caused exclusively by a single dynamic load case (i.e. under a single moving load or a specific seismic event).

While the interaction between moving loads and bridge systems has been widely investigated (e.g. Ichikawa et al. 2000; Xia et al. 2003; Xu et al. 2010; Salcher and Adam 2015; Ticona Melo et al. 2018; Xia et al. 2018; Zhang J et al. 2018), there are very limited studies on the structural response of bridge systems under simultaneous effects of moving loads and earthquake excitations (Wibowo et al. 2013; Nguyen 2015; Paraskeva et al. 2017). In one of the early studies, Yau (2009) developed a method to obtain the dynamic response of suspended beams subjected to simultaneous actions of moving vehicles and support excitations by decoupling the response into the pseudo-static and inertia-dynamic components. Using a similar approach, Frýba and Yau (2009) as well as Liu et al. (2011) studied the effects of simultaneous actions of moving loads and seismic excitations on the vibration of suspension bridges. It was shown that the interaction between the moving force and the vertical support excitation could considerably amplify the dynamic response of the bridge, especially in the event of high vehicle speeds. Emphasizing on the importance of incorporating the effects of vertical components of ground motions, Legeron and Sheikh (2009) proposed a methodology to determine the response of the bridge supports under vertical seismic loads. In contrast to the general design code requirements, they demonstrated that the effects of vertical seismic excitations should not be disregarded in the design process of bridges. This conclusion is in agreement with the results presented by other researchers (Saadeghvaziri and Foutch 1989; Papazoglou and Elnashai 1996; Wang T et al. 2105; Chen et al. 2016; Yang et al. 2015; Shrestha B 2015).

Several research studies have investigated the dynamic behaviour of single-span bridge systems under seismic ground motions by mainly focusing on the horizontal acceleration components (e.g. Ahmadi 1978; Su and Ahmadi 1988; Legeron and Sheikh 2009; Wang T et al. 2105; Yang et al. 2015; Shrestha B 2015; Chen et al. 2016). Zarfam et al. (2013) developed a method to assess the influence of the weight and velocity of traversing masses on the dynamic response of a beam subjected to horizontal support excitations at different frequencies. In other relevant studies, Konstantakopoulos et al. (2012) and Nguyen et al. (2017) analysed the vertical and horizontal dynamic response of suspension bridges subjected to earthquake and moving loads acting either separately or simultaneously. They concluded that the structural responses are significantly affected by the simultaneous effects of moving and seismic loads, especially when the moving loads are relatively small. However, the convective accelerations and the inertial acts of the moving vehicles were disregarded in most of the above-mentioned studies.

Elias and Matsagar (2017) developed a modified modal analysis approach to investigate the effectiveness of tuned mass dampers on isolated RC bridges including soil-structure interaction under horizontal earthquake excitations. A similar approach was then adopted by Matin et al. (2019) to study the effectiveness of distributed multiple tuned mass dampers in seismic response control of bridges under two horizontal components of earthquake ground motions. The main advantage of the modified modal analysis approach is that it can be used to obtain the response of non-classically damped systems.

Agrawal et al. (2009) and Tan and Agrawal (2009) presented the problem definition of a comprehensive benchmark structural control problem for the highway bridges under seismic excitations simultaneously applied in two directions. While different passive, semi-active and active devices and algorithms can be used to study the response of the benchmark model, the effects of moving masses (or vehicales) are not taken into account. Also the benchmark control systems are based on 3D detailed finite-element models, and therefore, can be computationally expensive.

Since the occurrence of an earthquake during the operational time of a bridge (i.e. whilst carrying moving loads) is highly likely, the structural response of the bridge system under such loading condition has to be adequately assessed during the design process. However, existing studies on the interaction between the vertical earthquake excitations and vehicle loads are commonly limited to the investigation of suspension bridges under moving forces (Frýba and Yau 2009; Liu et al. 2011; Konstantakopoulos et al. 2012; Nguyen et al. 2017). Therefore, more studies are required to extend the results to the general bridge systems. This is particularly important for the case where the moving mass is significant or is travelling at a high velocity (Nikkhoo et al. 2015).

In this paper dynamic behaviour of bridges under the simultaneous effects of moving inertial loads/vehicles and excitation due to the vertical component of earthquake excitations is investigated by adopting a modal analysis approach on simply-supported beams representing typical bridge systems. In addition, it is attempted to assess the efficiency of pipe dampers, originally proposed by Maleki and Bagheri (2010), to mitigate the vibrations induced by simultaneous actions of earthquake and vehicle loads on the beam-type bridge systems. To this end, the vertical acceleration component of seven near field earthquake ground motions with different frequency contents is applied to a simply supported Euler-Bernoulli beam subjected to vehicle loads (or lumped masses) travelling at uniform intervals. The pipe dampers are then employed in the locations where maximum deflections commonly occur, aiming to evaluate their efficiency for mitigation of the vertical vibrations the bridge systems with different flexural rigidities. It is shown that if the number and configuration of the pipe dampers are optimally selected, the required structural weight of the main load-bearing components to satisfy a predefined preference target can be significantly reduced.

2. Problem Formulations

It is assumed that a uniform undamped single-span Euler-Bernoulli beam of length L undergoes a dynamic excitation $f(x,t)$. The Cartesian system adopted for the analysis is illustrated in Figure 1. Given $D(x,t)$ as

the function describing the vertical displacement along the beam at time t, the governing vibration equation is written as follows (Frýba 1999):

$$\rho A \frac{\partial^2 D(x,t)}{\partial t^2} + EI \frac{\partial^4 D(x,t)}{\partial x^4} = f(x,t) \tag{1}$$

where EI and ρA are the flexural rigidity and the mass per unit length of the beam, respectively. $f(x,t)$ is obtained by combining the results of i) a set of moving masses, m_k, spaced at uniform intervals d, and traversing the beam at a constant velocity of v, and ii) base excitation due to the vertical acceleration of the design earthquake $\frac{d^2 U_g(t)}{dt^2}$, resulting in the following equation (Ahmadi 1978; Yang et al. 1997):

$$f(x,t) = \sum_{k=1}^{N} m_k [g - \frac{d^2 D_0(t)}{dt^2}].U_k - \left\{ \rho A + \sum_{k=1}^{N} m_k U_k \right\}.\frac{d^2 U_g(t)}{dt^2} \tag{2}$$

where, by letting $\Delta H(t) = H(t - t_k) - H(t - t_k - L/v)$,

$$U_k = \delta [x - v(t - t_k)].\Delta H(t) . \tag{3}$$

Here, δ and $H(.)$ denote the Dirac delta and the unit step function, respectively. t_k represents the arrival time of the kth mass at the beam (i.e. $t_k = (k-1)d/v$), and N is the total number of moving masses. The action of the kth moving mass is considered via $H(t - t_k)$ function when the load enters the beam and deactivated through $H(t - t_k - L/v)$ when the load departures the beam. In Equation (2), $D_0(t)$ represents the vertical displacement of a moving mass. Given the fact that the moving masses are not separated from the beam surface during the course of vibration (i.e., $D_0(t) = D(x = v(t - t_k), t)$), the following equation is obtained:

$$\frac{d^2 D_0(t)}{dt^2} = \left\{ \frac{\partial^2 D(x,t)}{\partial t^2} + 2v \frac{\partial^2 D(x,t)}{\partial x.\partial t} + v^2 \frac{\partial^2 D(x,t)}{\partial x^2} \right\}_{x=v(t-t_k)} . \tag{4}$$
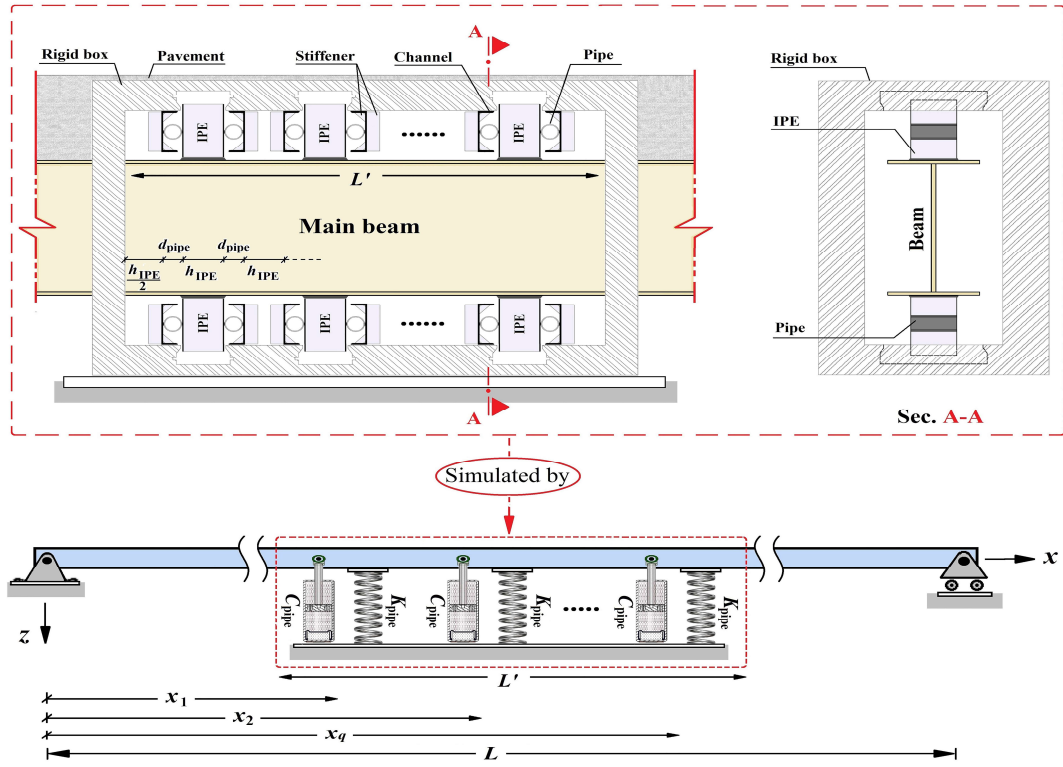
Figure 1. Schematic view of the steel pipe dampers along the main beam

3.   Formulation of the Steel Pipe Damper System

3.1. Definitions, assumptions and governing equations

In structural engineering, dampers are widely used to mitigate maximum vibrations under dynamic loads (e.g. moving load, wind or earthquake events) by dissipating the input energy transmitted to the structure. While different types of dampers have been successfully utilized for vibration control of bridges, experimental and analytical studies conducted by Maleki and Bagheri (2010) indicated that steel pipe damper can provide very efficient design solutions by offering a stable hysteresis behaviour and high energy absorption through metallic yielding. Therefore, in this study this type of damper is selected to mitigate the effects of simultaneous action of vertical earthquake excitation and vehicle loads in bridges. The mathematical formulation for application of steel pipe dampers is developed in the following section.

Figure 1 shows the schematic view of the steel pipe dampers installed along the main bridge beam. Stiffness factor of each pipe (K_{pipe}) in elastic and plastic deformation zones varies in proportional to the selected pipe. Maleki and Bagheri (2010) showed that the damping ratio of the system is defined as $\xi = E_D / (4\pi E_S)$. E_D is the overall energy absorbed by the dampers, which is equal to the area under the hysteresis load-displacement curve for one complete cycle. Finally, E_S represents the elastic strain energy of the pipes. Hence, damping factor of each pipe damper could be obtained as $C_{\text{pipe}} = 2\xi (M_{\text{pipe}} K_{\text{pipe}})^{1/2}$,

where M_{pipe} is the mass of each pipe in kilograms (kg). At each loading phase, the pipe dampers may enter the plastic phase while the beam itself is designed to remain in the elastic regime under the design load conditions. The experimental and analytical studies conducted by Maleki and Bagheri (2010) have demonstrated the good hysteresis behaviour and energy dissipation capacity of the steel pipe dampers. It should be noted that the dynamic systems solved in this study are considered to be classically damped since the damping matrix is orthogonal with respect to the modal vectors, and the stiffness and damping of the steel pipe dampers are only applied in one direction (Warburton and Soni 1977; Veletsos and Ventura 1986).

3.2. Configuration of the pipe damper system

As illustrated in Figure 1, the pipe damper system is a rigid box with length L', which is located at the mid-span of the bridge. The box comprises of a number of pipes with exterior diameter d_{pipe} connected to the main bridge beam by a European rolled steel section IPE. Placement of the pipe damper system is based on the fact that maximum deflection of a simply-supported beam under the assumed loading condition is expected to occur at the mid-span. The rigid box is assumed to respond completely isolated from the main beam, and therefore, does not impose any constraints on the beam deformation response under external excitation. For practical applications, depending on the location of the dampers and type of the bridge, the rigid box can be connected to the ground using a structural system such as a truss, pylon, concrete pad or pre-tensioned cables. It should be noted that while connecting the rigid box to the ground can slightly increase the constructional costs of the pipe damper system, the proposed system generally provides a more flexible and economic design solution than creating a structural pylon to convert the single span bridge to a multi-span system (Maleki and Bagheri (2010)).

As shown in Figure 1, the number of pipes attached above and below the main beam can be calculated as $q = n_{\text{pipe}} / 2$, where n_{pipe} is total number of pipes used in the box. Length of the rigid box is given by $L' = q \left[h_{\text{IPE}} + d_{\text{pipe}} \right]$, where h_{IPE} is depth of the IPE section used to connect the dampers to the main beam. Based on the bi-linear model presented by Maleki and Bagheri (2010), the response of the steel pipe damper system (rigid box) is simulated using a spring-dashpot by assuming $\Delta H(x) = H(x - x_1) - H(x - x_q)$, where x_1 and x_q are the distance between centre of the first and last pipe-couple from the assumed origin, respectively (see Figure 1).

$$
\begin{cases}
x_1 = \dfrac{L - L'}{2} + (h_{\text{IPE}} + d_{\text{pipe}}) \\
x_q = \dfrac{L + L'}{2} - (h_{\text{IPE}} + d_{\text{pipe}})
\end{cases}, \tag{5}
$$

The stiffness and damping of the steel pipes directly contribute to the beam vibration formula (Eq. (1)) as follows:

$$\rho A \frac{\partial^2 D(x,t)}{\partial t^2} + EI \frac{\partial^4 D(x,t)}{\partial x^4} + K_{\text{pipe}}^e D(x,t)\Delta H(x) = f(x,t) - C_{\text{pipe}}^e \frac{\partial D(x,t)}{\partial t}\Delta H(x), \tag{6}$$

in which, the equivalent stiffness and damping factors of the steel pipe system are calculated by the equations below:

$$\begin{cases} K_{\text{pipe}}^e = n_{\text{pipe}} . K_{\text{pipe}} \big/ (L' - h_{\text{IPE}}) \\ C_{\text{pipe}}^e = n_{\text{pipe}} . C_{\text{pipe}} \big/ (L' - h_{\text{IPE}}) \end{cases}. \tag{7}$$

Based on the above equation, K_{pipe}^e and C_{pipe}^e are the function of the stiffness and damping factors of steel pipes. Thus, they change proportionally to the pipe's elasto-plastic behaviour and do not possess a constant value during the course of vibration in the beam.

3.3. Spatial and time discretization of the governing equations

In this study, the Eigenfunction Expansion Method (EEM) is adopted to solve the above mentioned differential equation, as follows:

$$D(x,t) = \sum_{i=1}^{\infty} \varphi_i(x) a_i(t) \approx \sum_{i=1}^{p} \varphi_i(x) a_i(t) \tag{8}$$

where $\varphi_i(x)$ and $a_i(x)$ respectively denote the orthogonal shape function related to the ith beam vibration mode (in this study: $\varphi_i(x) = \sqrt{2/L}\sin(in\pi x/L)$; n = number of spans of the simply supported beams), and the corresponding i^{th} time-dependent amplitude. p is the total number of shape functions required to reach the predefined target accuracy. By substituting Eq. (8) into Eq. (6), multiplying both sides of the resulting equation by $\varphi_j(x)$, and lastly, integrating them over the length of the beam, the following equation is attained:

$$\begin{aligned}
& \rho A \sum_{i=1}^{p} \left\{ \sum_{j=1}^{p} \int_0^L \varphi_i(x)\varphi_j(x)\,dx \right\} \frac{\partial^2 a_i(t)}{\partial t^2} + EI \sum_{i=1}^{p} \left\{ \sum_{j=1}^{p} \int_0^L \frac{\partial^4 \varphi_i(x)}{\partial x^4}\varphi_j(x)\,dx \right\} a_i(t) \\
& + K_{\text{pipe}}^e \sum_{i=1}^{p} \left\{ \sum_{j=1}^{p} \int_{x_1}^{x_q} \varphi_i(x)\varphi_j(x)\,dx \right\} \Delta H(x) a_i(t) + C_{\text{pipe}}^e \sum_{i=1}^{p} \left\{ \sum_{j=1}^{p} \int_{x_1}^{x_q} \varphi_i(x)\varphi_j(x)\,dx \right\} \Delta H(x) \frac{\partial a_i(t)}{\partial t} \\
& = \sum_{k=1}^{N} \sum_{i=1}^{p} \sum_{j=1}^{p} m_k \int_0^L \left\{ g - \left[\varphi_i(x)\frac{\partial^2 a_i(t)}{\partial t^2} + 2v \frac{\partial \varphi_i(x)}{\partial x}\frac{\partial a_i(t)}{\partial t} + v^2 \frac{\partial^2 \varphi_i(x)}{\partial x^2} a_i(t) \right] \right\} \\
& \times \varphi_j(x).\delta[x - v(t - t_k)].\Delta H(t)\,dx - \frac{d^2 U_g(t)}{dt^2} \sum_{j=1}^{p} \int_0^L \varphi_j(x) \left\{ \rho A + \sum_{k=1}^{N} m_k .\delta[x - v(t - t_k)].\Delta H(t) \right\} dx .
\end{aligned} \tag{9}$$

By defining ω_i as the ith beam's natural frequency, the beam's free vibration equation can be presented as:

$$EI\int_0^L \frac{\partial^4 \varphi_i(x)}{\partial x^4}\varphi_j(x)\,dx = \rho A \omega_i^2 \int_0^L \varphi_i(x)\varphi_j(x)\,dx. \tag{10}$$

According to the orthogonality of the modes, i.e.

$$\langle \varphi_i(x), \varphi_j(x) \rangle = \int_0^L \varphi_i(x)\varphi_j(x)\,dx = \delta_{ij} = \begin{cases} 0 & \text{if} \quad i \neq j \\ 1 & \text{if} \quad i = j \end{cases} \quad ; \quad i,j = 1,2,...,p \tag{11}$$

and by substituting the Eq. (10) into the Eq. (9), the matrix form of Eq. (9) is rewritten as:

$$M(t)\frac{d^2 a(t)}{dt^2} + C(t)\frac{d a(t)}{dt} + K(t)a(t) = F(t), \tag{12}$$

in which

$$\mathbf{a}(t) = \left[a_i(t) \right]_{p\times 1}, \tag{13-1}$$

$$M(t) = \left[\rho A \delta_{ij} + \sum_{k=1}^N m_k \varphi_i[v(t-t_k)]\cdot\varphi_j[v(t-t_k)]\cdot\Delta H(t) \right]_{p\times p}, \tag{13-2}$$

$$C(t) = \Big[C_{\text{pipe}}^e \int_{x_1}^{x_q} \varphi_i(x)\varphi_j(x)\,dx\cdot\Delta H(x)$$
$$+ \sum_{k=1}^N 2m_k v\varphi_{i,x}[v(t-t_k)]\cdot\varphi_j[v(t-t_k)]\cdot\Delta H(t) \Big]_{p\times p}, \tag{13-3}$$

$$K(t) = \Big[\rho A \omega_i^2 \delta_{ij} + K_{\text{pipe}}^e \int_{x_1}^{x_q} \varphi_i(x)\varphi_j(x)\,dx\cdot\Delta H(x)$$
$$+ \sum_{k=1}^N m_k v^2 \varphi_{i,xx}[v(t-t_k)]\cdot\varphi_j[v(t-t_k)]\cdot\Delta H(t) \Big]_{p\times p}, \tag{13-4}$$

$$F(t) = \Big[[g - \frac{d^2 U_g(t)}{dt^2}]\sum_{k=1}^N m_k \varphi_j[v(t-t_k)]\cdot\Delta H(t) - \rho A \frac{d^2 U_g(t)}{dt^2}\int_0^L \varphi_j(x)\,dx \Big]_{p\times 1}. \tag{13-5}$$

By transforming Eq. (12) into a state-space form, the second order ODEs set in Eq. (12) could be reduced to a first order set of equations via the following reformulation:

$$\frac{d}{dt}\mathbf{X}(t) = \mathbf{A}(t)\mathbf{X}(t) + \mathbf{B}(t), \tag{14}$$

where

$$X(t) = \begin{bmatrix} a(t) \\ d\,a(t)/dt \end{bmatrix}_{2p\times 1}, \quad A(t) = \begin{bmatrix} 0_{p\times p} & I_{p\times p} \\ -M^{-1}K & -M^{-1}C \end{bmatrix}_{2p\times 2p}, \quad B(t) = \begin{bmatrix} 0_{p\times 1} \\ M^{-1}F \end{bmatrix}_{2p\times 1}. \tag{15}$$

A number of methods are available to solve Eq. (14) in the time domain. In this paper, the matrix-exponential method, proposed by Brogan (1985) and utilized by a number of other researchers (e.g. Ebrahimzadeh Hassanabadi et al. 2014; Niaz and Nikkhoo 2015; Nikkhoo 2014; Nikkhoo et al. 2014) is adopted for calculation of the displacement field. In the following section, the efficiency of the method is demonstrated through a benchmark numerical example.

4. Numerical Example

In this benchmark example, it is assumed that a group of moving vehicles are crossing a simply-supported bridge with a span length of $L = 60$ m (Legeron and Sheikh 2009). The deck of the bridge is supported by a number of beams parallel to the direction of the bridge. To analyse the vibration and maximum deformation of the bridge, one of the main beams, as indicated in Figure 2, is considered. According to Legeron and Sheikh (2009), the mechanical properties of the beam section are assumed as $EI = 3.467 \times 10^{10}$ N m^2 and $\rho A = 2956$ kg/m. The moving vehicles consist of a group of $m = 50000$ kg masses travelling with a constant velocity of $v = 30$ m/s and effective distance of d. As illustrated in Figure 2, it is assumed that when a traversing mass reaches the mid-span, the next mass enters the beam (i.e. $d = L/2$). This system is analysed for the first 16 seconds implying that, in total, 15 masses traverse the beam. Additionally, it is assumed that as the first mass arrives at the beam (i.e., for $t = 0$), the beam undergoes a vertical excitation caused by an earthquake event.
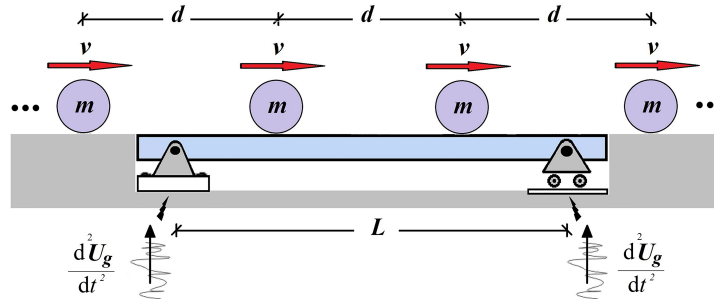
Figure 2. Schematic View of a simply-supported beam subjected to moving masses with uniform intervals

To investigate the effects of input ground motion characteristics on the dynamic response of the case study bridge system, the vertical acceleration records of seven major near field earthquakes are considered. The characteristics of the selected earthquakes are presented in Table 1 (PEER center). The soil conditions corresponding to the selected earthquake records based on SEI/ASCE 7-16 classifications are also shown in Table 1. It can be seen that these earthquake records are chosen in a way to cover different soil types and fault mechanisms. Figure 3 compares the acceleration response spectrum of the selected earthquake records.

Table 1. Earthquake Characteristics

Number	1	2	3	4	5	6	7
Event	L'Aquila, Italy	Imperial Valley-02	Kobe, Japan	Mammoth Lakes-01	Loma Prieta	Northridge-01	Tabas, Iran
Year	2009	1940	1995	1980	1989	1994	1978
Station	GRAN SASSO	El Centro Array #9	KJMA	Convict Creek	Corralitos	Arleta - Nordhoff	Tabas
Magnitude	6.3	6.95	6.9	6.06	6.93	6.69	7.35
Mechanism	Normal	Strike slip	Strike slip	Normal Oblique	Reverse Oblique	Reverse	Reverse
D5-95 (S)	8.9	24.2	9.5	9.6	7.9	13.5	16.5
Rjb (km)	6.35	6.09	0.94	1.1	0.16	3.3	1.79
Rrup (km)	6.4	6.09	0.96	6.63	3.85	8.66	2.05
Vs30 (m/s)	488	213	312	382	462	298	767
Soil type	C	D	D	C	C	D	B
PGA (H)	0.150g	0.281g	0.834 g	0.442g	0.645g	0.345g	0.862g
PGA (V)	0.110g	0.178g	0.339g	0.387g	0.458g	0.552g	0.641g
H/V Ratio	1.36	1.58	2.46	1.14	1.41	0.63	1.34
PGV (H) cm/s	9.71	31.31	91.06	23.75	55.94	41.09	123.34
PGV (V) cm/s	4.42	8.61	40.35	21.10	19.50	17.99	40.90
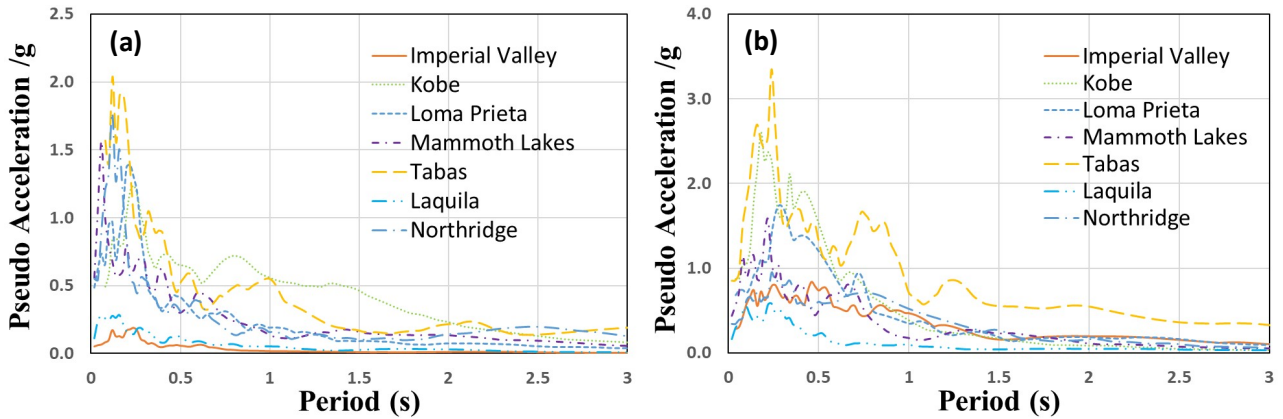
Figure 3. Response Spectrum of the selected earthquake ground motions; a) Vertical Components, b) Horizontal Components

4.1. Vertical Seismic Loads and their Interaction with Moving Inertial Loads

The mid-span beam deflection response of the case study bridge (Figure 2) due to the moving masses (dash line) and the simultaneous effects of moving masses and earthquake excitations (solid line) are depicted in Figure 4. As observed, in most cases, the seismic loads amplified the effects of moving vehicles and resulted in deflections up to twice the case excluding seismic actions. This effect was especially evident in Kobe and Tabas nearfield earthquakes with large vertical components (see Figure 3). For better comparison, Table 2 presents the maximum deflection at the beam's mid-span locations under the two above loading conditions. As it is seen, the discrepancies in responses vary for different earthquakes. The increase in the beam vertical deflection response due to the vertical component of the input earthquake is represented by M_n factor. It can be noticed that, on average, the vertical deflections increased by over 40% under simultaneous effect of moving mass and earthquake vertical excitations. These results clearly demonstrate the importance of considering the interaction of the vertical components of earthquakes and moving masses in the design of beam-like structures as will be discussed further in the following sections.
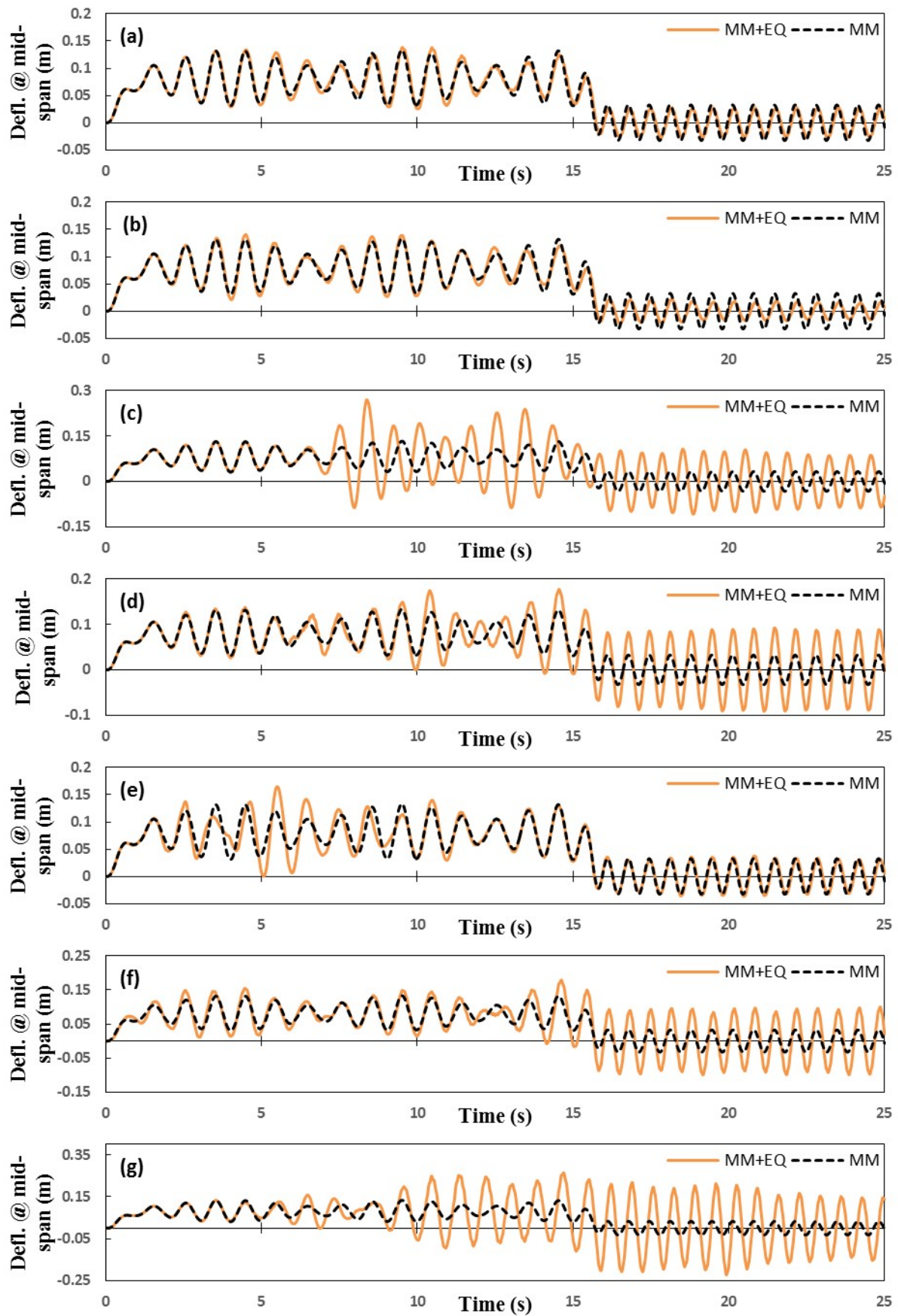
10

Figure 4. Time-history deflection of the beam due to external excitations a) L'Aquila, b) Imperial Valley, c) Kobe, d) Mammoth Lakes, e) Loma Prieta, f) Northridge, g) Tabas.

Table 2. Impact of vertical earthquake excitation on maximum deflections at beam's mid-span

Number	Earthquake Event	Maximum mid-span beam deflection (m)		Impact of vertical earthquake excitation on mid-span deflection M_n (%)
		Moving mass	Moving mass + Earthquake	
1	L'Aquila, Italy	0.133	0.138	3.8
2	Imperial Valley-02	0.133	0.141	6.0
3	Kobe, Japan	0.133	0.270	103
4	Mammoth Lakes-01	0.133	0.177	33.1
5	Loma Prieta	0.133	0.165	24.1
6	Northridge-01	0.133	0.180	35.3
7	Tabas, Iran	0.133	0.264	98.5

4.2. Efficiency of Steel Pipe Dampers in Vibration Suppression

The objective of this section is to assess the efficiency of the steel pipe dampers in mitigating the vibrations in the beam bridge system induced by simultaneous actions of moving masses and vertical seismic excitations. As in the study conducted by Maleki and Bagheri (2010), the exterior diameter of the pipe dampers was set to be $d_{\text{pipe}} = 119 \, \text{mm}$, while it was assumed that $E_D = 173 \, \text{kN mm}$ and $E_S = 34 \, \text{kN mm}$. The stiffness factor of each pipe (K_{pipe}) in elastic and plastic deformation zones are given by $0.0034l \, (\text{kN} / \text{mm})$ and $0.00017l \, (\text{kN} / \text{mm})$, respectively. Moreover, according to the bi-linear empirical formulation presented by Maleki and Bagheri (2010), the yield strength of the pipe dampers was estimated as $F_y = 0.0088l \, (\text{kN})$, where l is the length of each pipe in millimetres (mm). Based on these assumptions, the deformation corresponding to F_y is calculated as 2.6 mm. An IPE270 section with the depth and flange width of $h_{\text{IPE}} = 270 \, \text{mm}$ and $b_{\text{IPE}} = 135 \, \text{mm}$ (in accordance to European standard DIN) was used to connect the pipes to the main beam.

It should be mentioned that in this study, the practical length of the pipe box L' was selected to be equal to the sitting length of the beam (proportional to the beam's length). Therefore, for a beam length of 60 m, L' was considered to be maximum 3 m. Thus, the maximum number of pipe dampers for this case study example was set to be 16 (should be a multiple of four as shown in Figure 1).

4.2.1. Single span bridge

Figure 5 demonstrates the variations in the deflection of the beam's mid-span as a function of the initial flexural rigidity factor ($K_n = \{0.5, 0.6, ..., 1\} \, EI$) for the single span bridge excluding dampers ($n_{\text{pipe}} = 0$) and the one including 4, 8, 12 and 16 steel pipe dampers ($n_{\text{pipe}} = 4, 8, 12, 16$) under the seven different earthquake scenarios. The results in Figure 5 indicate that, as expected, in the bridge systems without dampers, the maximum deflection of the beam under all seven selected earthquakes decreases as the flexural

rigidity increases. In general, this effect is more prominent for the initial flexural rigidity factors, K_n, smaller than 0.8. However, it is shown that the maximum deflection of the bridge systems with steel pipe dampers can be considered to be practically independent of the initial flexural rigidity factor of the bridge. It can be noted by using 16 pipe dampers (only across 5% of the total beam length), the maximum response amplitude of the bridge was significantly (up to 75%) reduced, particularly for the systems with low initial flexural rigidity factors.

The base line in Figure 5 shows the maximum deflection at the beam's mid-span without pipe dampers (i.e. $K_n = 1$ and $n_{\text{pipe}} = 0$). The aim is to find the Initial Flexural Rigidity Factor K_n, at which the maximum deflection of the beam with pipe dampers reaches the base line level. The reduction of the K_n is mainly achieved by reducing the size of the beam sections (slenderness of the base beam is assumed to be constant). This implies that, for the same performance target, using pipe dampers can considerably reduce the required structural weight. It is worth mentioning that the weight of these dampers is generally less than 1% of the total beam's weight.

For better comparison, Table 3 shows the required initial flexural rigidity factor K_n for the bridge systems with 16 pipe dampers to exhibit the same maximum mid-span deflection as the initial beam ($K_n =1$, $n_{\text{pipe}} = 0$) under the seven earthquake records. It is shown that by using 16 pipe dampers, the flexural rigidity of the main beams can be reduced by up to 27% (on average 16%).

According to Table 3, the performance of the pipe dampers seems to be dependent on the two main parameters M_n and $V_s 30(m/s)$. In general, as expected, the efficiency of the dampers increased by increasing the effect of vertical earthquake excitation (M_n). Similarly, in case of stiff soils with high values of $V_s 30(m/s)$, the performance of pipe dampers seems to be more profound. Based on the results, these two parameters can affect the response of the system independently. For instance, in case of the L'Aquila earthquake, although the M_n is negligible, due to the soil type (high value of $V_s 30(m/s)$), pipe dampers could reduce the required flexural rigidity by 14%. In the opposite situation, under the Kobe earthquake with small value of $V_s 30(m/s)$ and high value of M_n, utilizing the pipe dampers resulted in 17% reduction in the K_n. In case of the Imperial valley, where both $V_s 30(m/s)$ and M_n were small, the efficiency of dampers was considerably less than the other earthquake scenarios. On the contrary, the pipe dampers exhibited their maximum efficiency (27% reduction in K_n) under Tabas seismic event, where both $V_s 30(m/s)$ and M_n values were maximum.
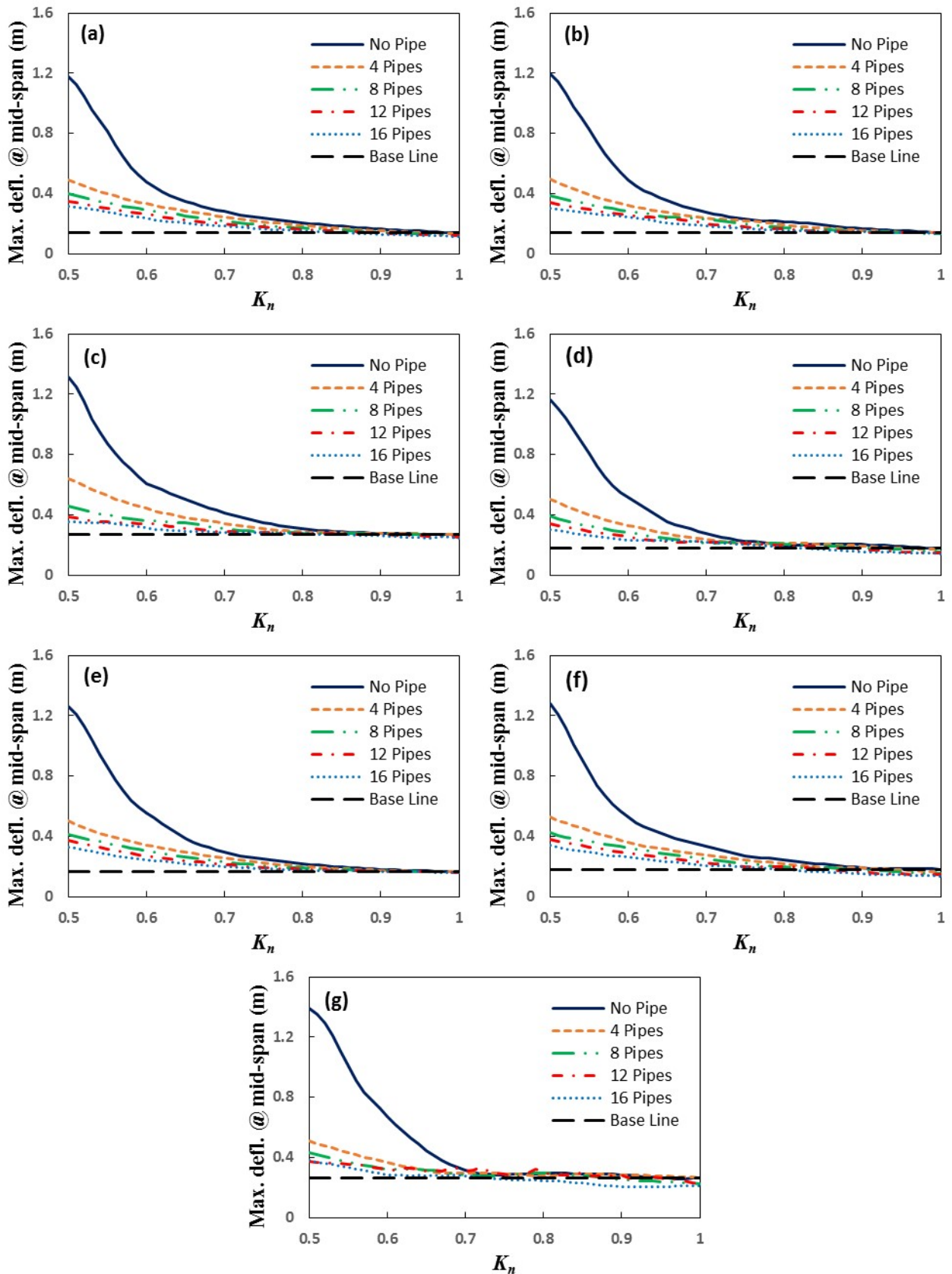
Figure 5. Effect of initial flexural rigidity factor K_n on the variations of the single span beam deflection with and without dampers a) L'Aquila, b) Imperial Valley, c) Kobe, d) Mammoth Lakes, e) Loma Prieta, f) Northridge, g) Tabas

The Fourier amplitude spectra curves illustrated in Figure 6 indicate that the dominant fundamental frequencies affecting the structural response of the beam system under different earthquake events do not change significantly after using pipe dampers.
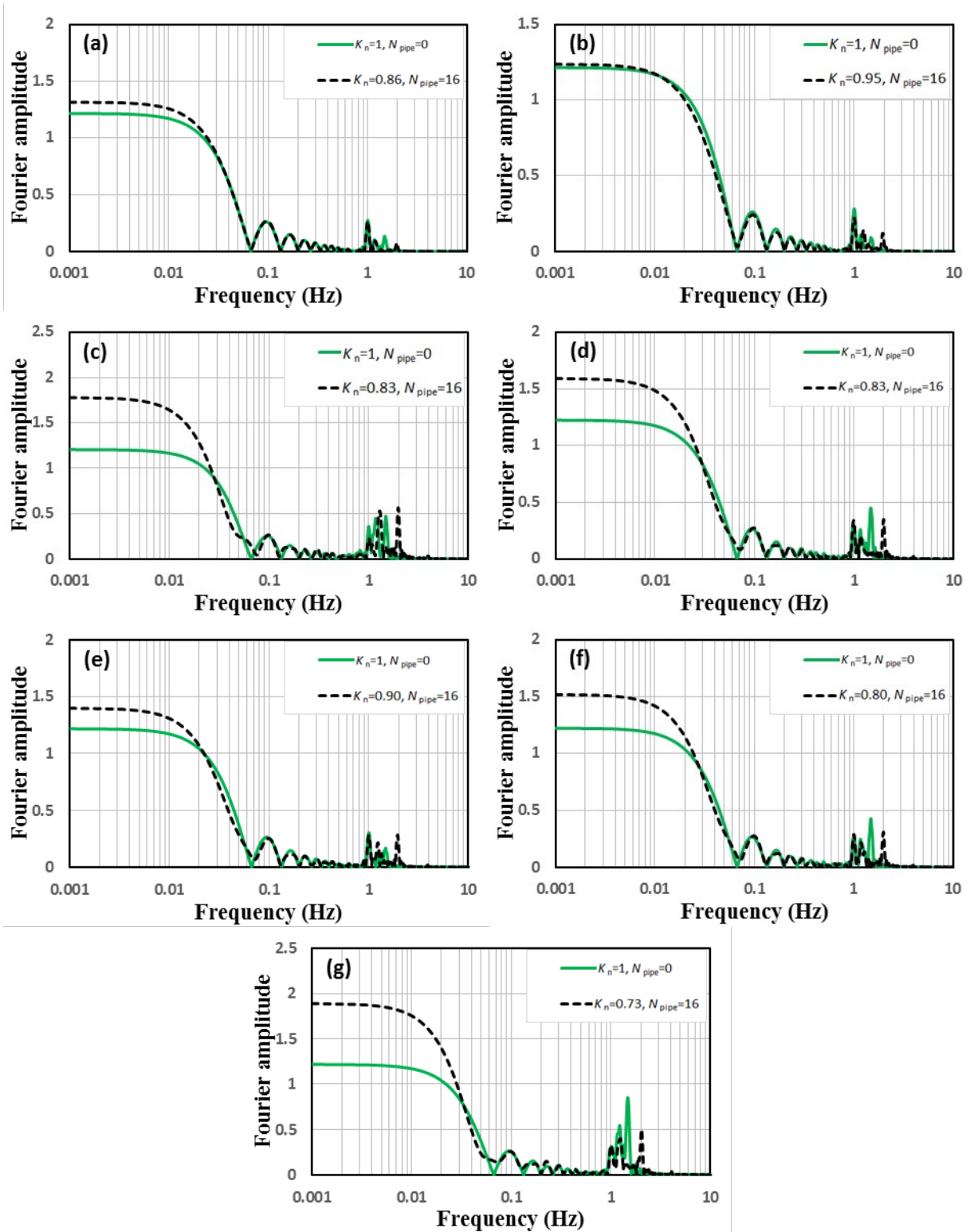

Figure 6. Effect of Frequency on the Fourier Amplitude of beam deflection with and without dampers a) L'Aquila K_n =0.86, b) Imperial Valley K_n =0.95, c) Kobe K_n =0.83, d) Mammoth Lakes K_n =0.83, e) Loma Prieta K_n =0.90, f) Northridge K_n =0.80, g) Tabas, K_n =0.73

Table 3. Effects of using steel pipe dampers and different initial flexural rigidity K_n on the maximum single span bridge deflection under the seven selected earthquakes

Number	Event	$V_s 30$ (m/s)	Effect of vertical earthquake M_n (%)	K_n	Number of pipe dampers	Maximum mid-span deflection (m)
1	L'Aquila, Italy	488	3.8	1	0	0.138
				0.86	16	
2	Imperial Valley	213	6.0	1	0	0.141
				0.95	16	
3	Kobe, Japan	312	103	1	0	0.270
				0.83	16	
4	Mammoth Lakes	382	33.1	1	0	0.177
				0.83	16	
5	Loma Prieta	462	24.1	1	0	0.165
				0.9	16	
6	Northridge	298	35.3	1	0	0.180
				0.8	16	
7	Tabas, Iran	766	98.5	1	0	0.264
				0.73	16	

4.2.2. Multiple span bridge

As indicated in Figure 7, a three-span bridge with simple ends and total length of $L = 180$ m (each span is 60 m) and $d = L/6$ is assumed. The pipe damper system is installed at the mid-span of each span (see Figure 7). The rest of the properties are the same as was assumed for the single span example.
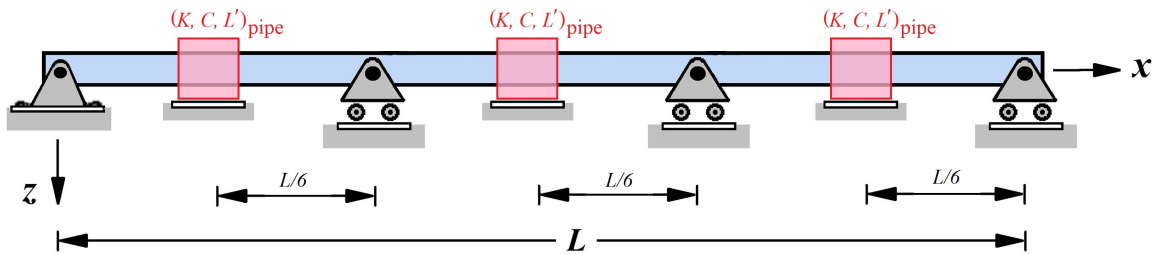

Figure 7. Schematic view of a three-span beam equipped with the pipe dampers system

Figure 8 illustrates the spectrum of the maximum deflection at the mid-span as a function of the initial flexural rigidity factor K_n. In addition, Table 4 shows the effects of using different number of steel pipe dampers and K_n on the maximum deflection of the three-span bridge example under the seven selected earthquakes.
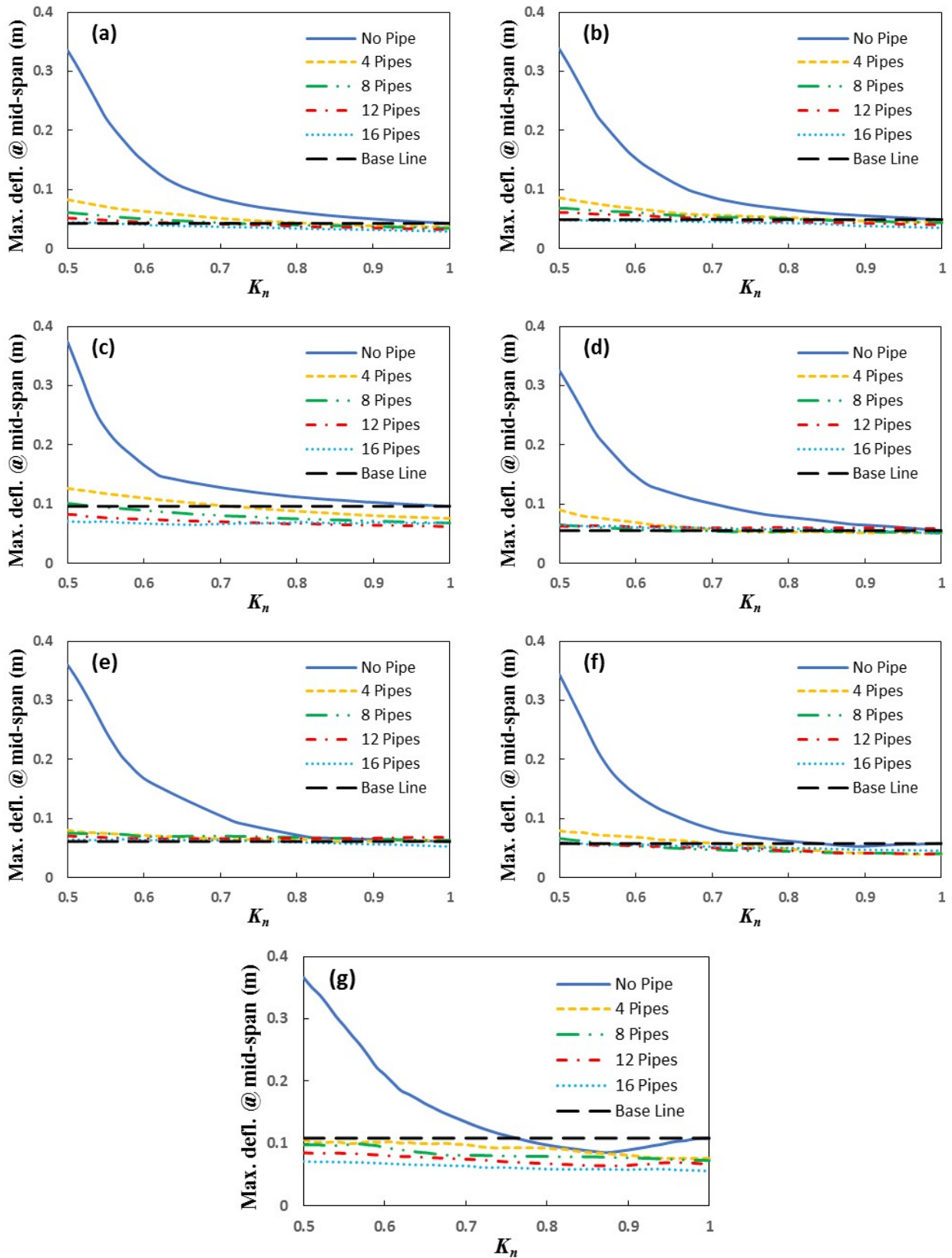
Figure 8. Effect of Initial Flexural Rigidity Factor K_n on the variations of three-span beam deflection with and without dampers a) L'Aquila, b) Imperial Valley, c) Kobe, d) Mammoth Lakes, e) Loma Prieta, f) Northridge, g) Tabas

Table 4. Effect of using different number of steel pipe dampers and Initial Flexural Rigidity K_n on the maximum deflection of three-span beam under seven selected earthquakes

Number	Event	$V_s 30$ (m/s)	Effect of vertical earthquake M_n (%)	K_n	Number of pipe dampers	Maximum mid-span deflection (m)
1	L'Aquila, Italy	488	5.0	1	0	0.045
				0.72	8	
2	Imperial Valley	213	8.8	1	0	0.049
				0.83	8	
3	Kobe, Japan	312	113.5	1	0	0.097
				0.54	8	
4	Mammoth Lakes	382	22.4	1	0	0.055
				0.64	8	
5	Loma Prieta	462	35.5	1	0	0.061
				0.77	8	
6	Northridge	298	28.1	1	0	0.058
				0.56	8	
7	Tabas, Iran	766	140.4	1	0	0.109
				0.5	8	

Similar to the single span bridge example, utilizing the pipe damper system could considerably improve the dynamic performance of the three-span bridge system in the range of variation of initial flexural rigidity factor K_n. However, it can be noticed that the efficiency of the pipe damper system was more prominent in the three-span bridge. This can be due to the higher values of M_n in the three span bridge compared to the single span example in most of the selected earthquake events, and also utilizing three packs of dampers for the three-span bridge system. The results in Table 4 indicate that by employing 8 pipe dampers, the flexural rigidity of the main beam can be reduced up to 50% (on average 35%) in the three-span bridge example.

5. Summary and Conclusions

This study aimed to thoroughly assess the vibration phenomenon and develop a mitigation technique for simply supported bridge systems subjected to simultaneous effects of moving vehicles and vertical earthquake ground motion. Through an extensive analytical study using the Eigenfunction Expansion Method (EEM), it was shown that if a near-field earthquake with a strong vertical component strikes while vehicles are travelling across the bridge, depending on the frequency content of the earthquake, displacement response of the bridge could be severely intensified (even by 100%). While the effects of vertical earthquake loads are usually ignored in the current design guidelines, this highlights the importance of considering the simultaneous effects of vertical earthquake excitation and vehicle loads in the design process of bridge systems in seismic regions. Subsequently, the efficiency of using steel pipe dampers were examined as a novel technique to mitigate the vibrations induced in single and multi-span simply-supported bridges. It was shown that the proposed system can significantly reduce the maximum response amplitude of the bridge (up to 75%) especially for the systems with low initial flexural rigidity factors. Regardless of the input earthquake characteristics, the maximum deflection of the bridge appeared to be less sensitive to the variations of flexural rigidity (commonly ties to environmental variations) when pipe dampers are employed

maximum deflection of the bridge appeared to be less sensitive to the variation of flexural rigidity (commonly ties to design uncertainties and environmental variations) when pipe dampers are employed. The results of this study indicated that the efficiency of pipe dampers generally improved by increasing the M_n and $V_s 30 (m/s)$ of the input earthquake. For the same maximum mid-span deflection limit, application of pipe dampers in bridges could reduce the required flexural rigidity of the single-span and multi-span systems by up to 27% and 50%, respectively, under the set of seven selected earthquake records. This implies that the proposed vibration mitigation method can potentially reduce the constructional costs by reducing the structural weight of the bridge system.

References

Agrawal AK, Tan P, Nagarajaiah S and Zhang J (2009), "Benchmark structural control problem for a seismically excited highway bridge - Part I: Phase I Problem definition," Struct. Control Health Monit., 16:509-529.

Ahmadi G (1978), "Earthquake response of linear continuous systems," *Nucl. Eng. Des.*, 50(2): 327-345.

American Railway Engineering and Maintenance-of-Way Association (AREMA) (1997), Part 1, "Design", Manual for Railway Engineering. American Railway, Engineering and Maintenance-of-Way Association, Lanham, MD, USA.

American Society of Civil Engineers (2017). SEI/ASCE 7-16. Minimum Design Loads for. Buildings and Other Structures, American Society of Civil Engineers

Beskou ND, Theodorakopoulos DD (2011) "Dynamic effects of moving loads on road pavements," *a review. Soil Dyn Earthq Eng*, 31(4): 547–567.

Brogan WL (1985), *Modern control theory*, Pearson Education India.

Chen YZ, Kun C, Larkin T and Chouw N (2016), "Impact of Vertical Ground Excitation on a Bridge with Footing Uplift," *J EARTHQ ENG*, 20(7): 1035–1053.

DIN 1025-5 (2014), Hot rolled l-beams, medium flange l-beams, IPE-serie, dimensions, masses, sectional properties.

Ebrahimzadeh Hassanabadi M, Vaseghi Amiri J and Davoodi M (2014), "On the vibration of a thin rectangular plate carrying a moving oscillator," *Sci. Iran.*, 21(2): 284-294.

Elias, S., & Matsagar, V. (2017). Effectiveness of tuned mass dampers in seismic response control of isolated bridges including soil-structure interaction. Latin American Journal of Solids and Structures, 14(13), 2324-2341

Frýba L (1999), *Vibration of solids and structures under moving loads*, Thomas Telford, London.

Frýba L and Yau JD (2009), "Suspended bridges subjected to moving loads and support motions due to earthquake," *J. Sound Vib.*, 319(1): 218-227.

He W (2018), "Vertical dynamics of a single-span beam subjected to moving mass-suspended payload system with variable speeds," *J. Sound Vib.*, 418: 36-54.

Ichikawa M, Miyakawa Y and Matsuda A (2000), "Vibration analysis of the continuous beam subjected to a moving mass," *J. Sound Vib.*, 230(3): 493-506.

Karimi AH, Ziaei-Rad S (2015), "Vibration analysis of a beam with moving support subjected to a moving mass travelling with constant and variable speed," *Commun Nonlinear Sci Numer Simul*, 29(1–3): 372-390.

Kiani K and Nikkhoo A (2012), "On the limitations of linear beams for the problems of moving mass-beam interaction using a meshfree method," *Acta Mech. Sin.*, 28(1): 164-179.

Konstantakopoulos T, Raftoyiannis I and Michaltsos G (2012), "Suspended bridges subjected to earthquake and moving loads," *Eng. Struct.*, 45: 223-237.

Legeron F and Sheikh MN (2009), "Bridge support elastic reactions under vertical earthquake ground motion," *Eng. Struct.*, 31(10): 2317-2326.

Leissa AW and Qatu MS (2011), *Vibration of continuous systems*, McGraw-Hill.

Liu M, Chang T and Zeng D (2011), "The interactive vibration behavior in a suspension bridge system under moving vehicle loads and vertical seismic excitations," *Appl. Math. Model.*, 35(1): 398-411.

Maleki S and Bagheri S (2010), "Pipe damper, Part I: Experimental and analytical study," *J. Constr. Steel Res.*, 66(8): 1088-1095.

Maleki S and Bagheri S (2010), "Pipe damper, Part II: Application to bridges," *J. Constr. Steel Res.*, 66(8): 1096-1106.

Matin, A., Elias, S., & Matsagar, V. (2019). Distributed multiple tuned mass dampers for seismic response control in bridges. Proceedings of the Institution of Civil Engineers-Structures and Buildings, 1-18

Maximov JT (2014), "A new approach to modeling the dynamic response of Bernoulli-Euler beam under moving load," *Coupled Syst. Mech.*, 3(3): 247-265.

Nguyen KV (2015), "Dynamic Analysis of a Cracked Beam-Like Bridge Subjected to Earthquake and Moving Vehicle," *ADV STRUCT ENG*, 18(1): 75-95.

Nguyen X-T, Tran V-D and Hoang N-D (2017), "An Investigation on the Dynamic Response of Cable Stayed Bridge with Consideration of Three-Axle Vehicle Braking Effects," *Journal of Computational Engineering*,2017, doi:org/10.1155/2017/4584657

Niaz M and Nikkhoo A (2015), "Inspection of a Rectangular Plate Dynamics Under a Moving Mass With Varying Velocity Utilizing BCOPs," *Lat. Am. J. Solids Struct., an ABCM Journal*, 12(2): 317-332.

Nikkhoo A (2014), "Investigating the behavior of smart thin beams with piezoelectric actuators under dynamic loads," *Mech. Syst. Signal Process.*, 45(2): 513-530.

Nikkhoo A, Ebrahimzadeh Hassanabadi M, Eftekhar Azam S and Vaseghi Amiri J (2014), "Vibration of a thin rectangular plate subjected to series of moving inertial loads," *Mech. Res. Commun.*, 55: 105-113.

Nikkhoo A, Farazandeh A and Ebrahimzadeh Hassanabadi M (2014), "On the computation of moving mass/beam interaction utilizing a semi-analytical method," *J. Braz. Soc. Mech. Sci. Eng.*, 38(3): 761-771.

Nikkhoo A, Farazandeh A, Ebrahimzadeh Hassanabadi M and Mariani S (2015), "Simplified modeling of beam vibrations induced by a moving mass by regression analysis," *Acta Mech.*, 226(7): 2147-2157.

Nikkhoo A, Rofooei FR and Shadnam M (2007), "Dynamic behavior and modal control of beams under moving mass," *J. Sound Vib.*, 306(3): 712-724.

Ouyang H (2011), "Moving-load dynamic problems: A tutorial (with a brief overview)," *Mech. Syst. Signal Process.*, 25(6): 2039-2060.

Papazoglou A and Elnashai A (1996), "Analytical and field evidence of the damaging effect of vertical earthquake ground motion," *Earthq. Eng. Struct. Dyn.*, 25(10): 1109-1138.

Paraskeva TS, Dimitrakopoulos EG, Zeng Q (2017), "Dynamic vehicle–bridge interaction under simultaneous vertical earthquake excitation," *Bull. Earthq. Eng.*, 15(1):71–95.

PEER center, "PEER Ground Motion Database," https://ngawest2.berkeley.edu/.

Pi Y, Ouyang H (2015), "Lyapunov-based boundary control of a multi-span beam subjected to moving masses," *J. Vib. Control.*, 23(14): 2221-2234.

Saadeghvaziri MA and Foutch DA (1989), "Effects of vertical motion on the inelastic behavior of highway bridges," *Proc., Seismic Engineering: Research and Practice*, ASCE, 51-61.

Salcher P, Adam C (2015), "Modeling of dynamic train–bridge interaction in high-speed railways," *Acta Mech* 226(8): 2473–2495.

Shrestha B (2015), "Seismic Response of Long Span Cable-stayed Bridge to Near-fault Vertical Ground Motions," *KSCE J CIV ENG*, 19(1): 180-187.

Su L and Ahmadi G (1988), "Earthquake response of linear continuous structures by the method of evolutionary spectra," *Eng. Struct.*, 10(1): 47-56.

Tan P and Agrawal AK (2009), "Benchmark structural control problem for a seismically excited highway bridge - Part II: Phase I Sample control designs," Struct. Control Health Monit., 16:530-548.

The European Standard EN 1991-2: Eurocode 1: Actions on structures –Part 2: Traffic Loads on Bridges, European Standard: CEN-Cenelec (www. cenelec.eu), Brussels, 1991.

Ticona Melo LR, Bittencourt TN, Ribeiro D, Calçada R (2018), "Dynamic Response of a Railway Bridge to Heavy Axle-Load Trains Considering Vehicle–Bridge Interaction," International Journal of Sttrucutral Stability and Dynamics ,18(1).

Union Internationale des Chemins de Fer, UIC Code 776-2 R: Design requirements for rail-bridges in particular speed, 2002.

Veletsos AS, Ventura CE (1986), "Modal analysis of non-classically damped linear systems," Earthquake Engineering and Structural Dynamics, 14: 217-243.

Wang T, Li H, Ge Y (2015), "Vertical seismic response analysis of straight girder bridges considering effects of support structures," *Earthquakes and Structures*, 8(6): 1481-1497.

Wang T, Li H, Ge Y (2015), "Vertical seismic response analysis of straight girder bridges considering effects of support structures," *Earthquakes and Structures*, 8(6):1481-1497.

Warburton GB, Soni SR (1977), "Errors in Response Calculations for Non-Classically Damped Structures," Earthquake Engineering and Structural Dynamics, 5. 365 - 376.

Wibowo H, Sanford DM, Buckle IG and Sanders DH (2013), "Effect of live load on the seismic response of bridges," Department of transportation, (No. CCEER 13-10), California.

Xia H, Zhang N and De Roeck G (2003), "Dynamic analysis of high speed railway bridge under articulated trains," *Comput. struct.*, 81(26): 2467-2478.

Xia H, Zhang N, Guo W (2018), "Dynamic Analysis of Train-Bridge Coupling System," Dynamic Interaction of Train-Bridge Systems in High-Speed Railways. Advances in High-speed Rail Technology. Springer, Berlin, Heidelberg.

Xu Y, Li Q, Wu D and Chen Z (2010), "Stress and acceleration analysis of coupled vehicle and long-span bridge systems using the mode superposition method," *Eng. Struct.*, 32(5): 1356-1368.

Yang H, Yin X, Hao H and Bi K (2015), "Theoretical Investigation of Bridge Seismic Responses with Pounding under Near-Fault Vertical Ground Motions," *ADV STRUCT ENG* , 18(4): 453-468.

Yang J, Ouyang H, Stancioiu D (2017), "Numerical Studies of Vibration of Four-Span Continuous Plate with Rails Excited by Moving Car with Experimental Validation," *Int. J. Str. Stab. Dyn.*, 17(10).

Yang YB, Yau JD and Hsu LC (1997), "Vibration of simple beams due to trains moving at high speeds," *Eng. struct.*, 19(11): 936-944.

Yau J (2009), "Dynamic response analysis of suspended beams subjected to moving vehicles and multiple support excitations," *J. Sound Vib.*, 325(4): 907-922.

Zarfam R, Khaloo AR and Nikkhoo A (2013), "On the response spectrum of Euler-Bernoulli beams with a moving mass and horizontal support excitation," *Mech. Res. Commun.*, 47: 77-83.

Zhang J, Gao Q, Wu F, Zhong W-X (2018), "A linear complementarity method for the solution of vertical vehicle–track interaction," *VEHICLE SYST DYN*, 56(2): 281-296.

Zhu DY, Zhang YH, Ouyanga H (2015), "A linear complementarity method for dynamic analysis of bridges under moving vehicles considering separation and surface roughness," *Comput. struct.*, 154(1) :135-144.